

Measurement of the inclusive isolated prompt photon cross section in $p\bar{p}$ collisions at $\sqrt{s} = 1.96$ TeV using the CDF detector

T. Aaltonen,²⁴ J. Adelman,¹⁴ B. Álvarez González,^{12,w} S. Amerio,^{44b,44a} D. Amidei,³⁵ A. Anastassov,³⁹ A. Annovi,²⁰ J. Antos,¹⁵ G. Apollinari,¹⁸ A. Apresyan,⁴⁹ T. Arisawa,⁵⁸ A. Artikov,¹⁶ J. Asaadi,⁵⁴ W. Ashmanskas,¹⁸ A. Attal,⁴ A. Aurisano,⁵⁴ F. Azfar,⁴³ W. Badgett,¹⁸ A. Barbaro-Galtieri,²⁹ V. E. Barnes,⁴⁹ B. A. Barnett,²⁶ P. Barria,^{47c,47a} P. Bartos,¹⁵ G. Bauer,³³ P.-H. Beauchemin,³⁴ F. Bedeschi,^{47a} D. Beecher,³¹ S. Behari,²⁶ G. Bellettini,^{47b,47a} J. Bellinger,⁶⁰ D. Benjamin,¹⁷ A. Beretvas,¹⁸ A. Bhatti,⁵¹ M. Binkley,¹⁸ D. Bisello,^{44b,44a} I. Bizjak,^{31,dd} R. E. Blair,² C. Blocker,⁷ B. Blumenfeld,²⁶ A. Bocci,¹⁷ A. Bodek,⁵⁰ V. Boisvert,⁵⁰ D. Bortoletto,⁴⁹ J. Boudreau,⁴⁸ A. Boveia,¹¹ B. Brau,^{11,b} A. Bridgeman,²⁵ L. Brigliadori,^{6b,6a} C. Bromberg,³⁶ E. Brubaker,¹⁴ J. Budagov,¹⁶ H. S. Budd,⁵⁰ S. Budd,²⁵ K. Burkett,¹⁸ G. Busetto,^{44b,44a} P. Bussey,²² A. Buzatu,³⁴ K. L. Byrum,² S. Cabrera,^{17,y} C. Calancha,³² S. Camarda,⁴ M. Campanelli,³⁶ M. Campbell,³⁵ F. Canelli,^{14,18} A. Canepa,⁴⁶ B. Carls,²⁵ D. Carlsmith,⁶⁰ R. Carosi,^{47a} S. Carrillo,^{19,o} S. Carron,¹⁸ B. Casal,¹² M. Casarsa,¹⁸ A. Castro,^{6b,6a} P. Catastini,^{47c,47a} D. Cauz,^{55a} V. Cavaliere,^{47c,47a} M. Cavalli-Sforza,⁴ A. Cerri,²⁹ L. Cerrito,^{31,r} S. H. Chang,²⁸ Y. C. Chen,¹ M. Chertok,⁸ G. Chiarelli,^{47a} G. Chlachidze,¹⁸ F. Chlebana,¹⁸ K. Cho,²⁸ D. Chokheli,¹⁶ J. P. Chou,²³ G. Choudalakis,³³ K. Chung,^{18,p} W. H. Chung,⁶⁰ Y. S. Chung,⁵⁰ T. Chwalek,²⁷ C. I. Ciobanu,⁴⁵ M. A. Ciocci,^{47c,47a} A. Clark,²¹ D. Clark,⁷ G. Compostella,^{44a} M. E. Convery,¹⁸ J. Conway,⁸ M. Corbo,⁴⁵ M. Cordelli,²⁰ C. A. Cox,⁸ D. J. Cox,⁸ F. Crescioli,^{47b,47a} C. Cuenca Almenar,⁶¹ J. Cuevas,^{12,w} R. Culbertson,¹⁸ J. C. Cully,³⁵ D. Dagenhart,¹⁸ M. Datta,¹⁸ T. Davies,²² P. de Barbaro,⁵⁰ S. De Cecco,^{52a} A. Deisher,²⁹ G. De Lorenzo,⁴ M. Dell'Orso,^{47b,47a} C. Deluca,⁴ L. Demortier,⁵¹ J. Deng,^{17,g} M. Deninno,^{6a} M. d'Errico,^{44b,44a} A. Di Canto,^{47b,47a} G. P. di Giovanni,⁴⁵ B. Di Ruzza,^{47a} J. R. Dittmann,⁵ M. D'Onofrio,⁴ S. Donati,^{47b,47a} P. Dong,¹⁸ T. Dorigo,^{44a} S. Dube,⁵³ K. Ebina,⁵⁸ A. Elagin,⁵⁴ R. Erbacher,⁸ D. Errede,²⁵ S. Errede,²⁵ N. Ershaidat,^{45,cc} R. Eusebi,⁵⁴ H. C. Fang,²⁹ S. Farrington,⁴³ W. T. Fedorko,¹⁴ R. G. Feild,⁶¹ M. Feindt,²⁷ J. P. Fernandez,³² C. Ferrazza,^{47d,47a} R. Field,¹⁹ G. Flanagan,^{49,t} R. Forrest,⁸ M. J. Frank,⁵ M. Franklin,²³ J. C. Freeman,¹⁸ I. Furic,¹⁹ M. Gallinaro,⁵¹ J. Galyardt,¹³ F. Garberon,¹¹ J. E. Garcia,²¹ A. F. Garfinkel,⁴⁹ P. Garosi,^{47c,47a} K. Genser,¹⁸ H. Gerberich,²⁵ D. Gerdes,³⁵ A. Gessler,²⁷ S. Giagu,^{52b,52a} V. Giakoumopoulou,³ P. Giannetti,^{47a} K. Gibson,⁴⁸ J. L. Gimmell,⁵⁰ C. M. Ginsburg,¹⁸ N. Giokaris,³ M. Giordani,^{55b,55a} P. Giromini,²⁰ M. Giunta,^{47a} G. Giurgiu,²⁶ V. Glagolev,¹⁶ D. Glenzinski,¹⁸ M. Gold,³⁸ N. Goldschmidt,¹⁹ A. Golossanov,¹⁸ G. Gomez,¹² G. Gomez-Ceballos,³³ M. Goncharov,³³ O. González,³² I. Gorelov,³⁸ A. T. Goshaw,¹⁷ K. Goulianos,⁵¹ A. Gresele,^{44b,44a} S. Grinstein,⁴ C. Grosso-Pilcher,¹⁴ R. C. Group,¹⁸ U. Grundler,²⁵ J. Guimaraes da Costa,²³ Z. Gunay-Unalan,³⁶ C. Haber,²⁹ K. Hahn,³³ S. R. Hahn,¹⁸ E. Halkiadakis,⁵³ B.-Y. Han,⁵⁰ J. Y. Han,⁵⁰ F. Happacher,²⁰ K. Hara,⁵⁶ D. Hare,⁵³ M. Hare,⁵⁷ R. F. Harr,⁵⁹ M. Hartz,⁴⁸ K. Hatakeyama,⁵ C. Hays,⁴³ M. Heck,²⁷ J. Heinrich,⁴⁶ C. Henderson,³³ M. Herndon,⁶⁰ J. Heuser,²⁷ S. Hewamanage,⁵ D. Hidas,⁵³ C. S. Hill,^{11,d} D. Hirschbuehl,²⁷ A. Hocker,¹⁸ S. Hou,¹ M. Houlden,³⁰ S.-C. Hsu,²⁹ B. T. Huffman,⁴³ R. E. Hughes,⁴⁰ M. Hurwitz,¹⁴ U. Husemann,⁶¹ M. Hussein,³⁶ J. Huston,³⁶ J. Incandela,¹¹ G. Introzzi,^{47a} M. Iori,^{52b,52a} A. Ivanov,^{8,q} E. James,¹⁸ D. Jang,¹³ B. Jayatilaka,¹⁷ E. J. Jeon,²⁸ M. K. Jha,^{6a} S. Jindariani,¹⁸ W. Johnson,⁸ M. Jones,⁴⁹ K. K. Joo,²⁸ S. Y. Jun,¹³ J. E. Jung,²⁸ T. R. Junk,¹⁸ T. Kamon,⁵⁴ D. Kar,¹⁹ P. E. Karchin,⁵⁹ Y. Kato,^{42,n} R. Kephart,¹⁸ W. Ketchum,¹⁴ J. Keung,⁴⁶ V. Khotilovich,⁵⁴ B. Kilminster,¹⁸ D. H. Kim,²⁸ H. S. Kim,²⁸ H. W. Kim,²⁸ J. E. Kim,²⁸ M. J. Kim,²⁰ S. B. Kim,²⁸ S. H. Kim,⁵⁶ Y. K. Kim,¹⁴ N. Kimura,⁵⁸ L. Kirsch,⁷ S. Klimentenko,¹⁹ B. Knuteson,³³ K. Kondo,⁵⁸ D. J. Kong,²⁸ J. Konigsberg,¹⁹ A. Korytov,¹⁹ A. V. Kotwal,¹⁷ M. Krepis,²⁷ J. Kroll,⁴⁶ D. Krop,¹⁴ N. Krumnack,⁵ M. Kruse,¹⁷ V. Krutelyov,¹¹ T. Kuhr,²⁷ N. P. Kulkarni,⁵⁹ M. Kurata,⁵⁶ S. Kwang,¹⁴ A. T. Laasanen,⁴⁹ S. Lami,^{47a} S. Lammel,¹⁸ M. Lancaster,³¹ R. L. Lander,⁸ K. Lannon,^{40,v} A. Lath,⁵³ G. Latino,^{47c,47a} I. Lazzizzera,^{44b,44a} T. LeCompte,² E. Lee,⁵⁴ H. S. Lee,¹⁴ J. S. Lee,²⁸ S. W. Lee,^{54,x} S. Leone,^{47a} J. D. Lewis,¹⁸ C.-J. Lin,²⁹ J. Linacre,⁴³ M. Lindgren,¹⁸ E. Lipeles,⁴⁶ A. Lister,²¹ D. O. Litvintsev,¹⁸ C. Liu,⁴⁸ T. Liu,¹⁸ N. S. Lockyer,⁴⁶ A. Loginov,⁶¹ L. Lovas,¹⁵ D. Lucchesi,^{44b,44a} J. Lueck,²⁷ P. Lujan,²⁹ P. Lukens,¹⁸ G. Lungu,⁵¹ J. Lys,²⁹ R. Lysak,¹⁵ D. MacQueen,³⁴ R. Madrak,¹⁸ K. Maeshima,¹⁸ K. Makhoul,³³ P. Maksimovic,²⁶ S. Malde,⁴³ S. Malik,³¹ G. Manca,^{30,f} A. Manousakis-Katsikakis,³ F. Margaroli,⁴⁹ C. Marino,²⁷ C. P. Marino,²⁵ A. Martin,⁶¹ V. Martin,^{22,l} M. Martínez,⁴ R. Martínez-Ballarín,³² P. Mastrandrea,^{52a} M. Mathis,²⁶ M. E. Mattson,⁵⁹ P. Mazzanti,^{6a} K. S. McFarland,⁵⁰ P. McIntyre,⁵⁴ R. McNulty,^{30,k} A. Mehta,³⁰ P. Mehtala,²⁴ A. Menzione,^{47a} C. Mesropian,⁵¹ T. Miao,¹⁸ D. Mietlicki,³⁵ N. Miladinovic,⁷ R. Miller,³⁶ C. Mills,²³ M. Milnik,²⁷ A. Mitra,¹ G. Mitselmakher,¹⁹ H. Miyake,⁵⁶ S. Moed,²³ N. Moggi,^{6a} M. N. Mondragon,^{18,o} C. S. Moon,²⁸ R. Moore,¹⁸ M. J. Morello,^{47a} J. Morlock,²⁷ P. Movilla Fernandez,¹⁸ J. Müllenstädt,²⁹ A. Mukherjee,¹⁸ Th. Müller,²⁷ P. Murat,¹⁸ M. Mussini,^{6b,6a} J. Nachtman,^{18,p} Y. Nagai,⁵⁶ J. Naganoma,⁵⁶ K. Nakamura,⁵⁶ I. Nakano,⁴¹ A. Napier,⁵⁷ J. Nett,⁶⁰ C. Neu,^{46,aa} M. S. Neubauer,²⁵ S. Neubauer,²⁷ J. Nielsen,^{29,h} L. Nodulman,² M. Norman,¹⁰ O. Norriella,²⁵ E. Nurse,³¹ L. Oakes,⁴³ S. H. Oh,¹⁷ Y. D. Oh,²⁸ I. Oksuzian,¹⁹ T. Okusawa,⁴²

R. Orava,²⁴ K. Osterberg,²⁴ S. Pagan Griso,^{44b,44a} C. Pagliarone,^{55a} E. Palencia,¹⁸ V. Papadimitriou,¹⁸ A. Papaikononou,²⁷ A. A. Paramanov,² B. Parks,⁴⁰ S. Pashapour,³⁴ J. Patrick,¹⁸ G. Pauletta,^{55b,55a} M. Paulini,¹³ C. Paus,³³ T. Peiffer,²⁷ D. E. Pellett,⁸ A. Penzo,^{55a} T. J. Phillips,¹⁷ G. Piacentino,^{47a} E. Pianori,⁴⁶ L. Pinera,¹⁹ K. Pitts,²⁵ C. Plager,⁹ L. Pondrom,⁶⁰ K. Potamianos,⁴⁹ O. Poukhov,^{16,a} F. Prokoshin,^{16,z} A. Pronko,¹⁸ F. Ptohos,^{18,j} E. Pueschel,¹³ G. Punzi,^{47b,47a} J. Pursley,⁶⁰ J. Rademacker,^{43,d} A. Rahaman,⁴⁸ V. Ramakrishnan,⁶⁰ N. Ranjan,⁴⁹ I. Redondo,³² P. Renton,⁴³ M. Renz,²⁷ M. Rescigno,^{52a} S. Richter,²⁷ F. Rimondi,^{6b,6a} L. Ristori,^{47a} A. Robson,²² T. Rodrigo,¹² T. Rodriguez,⁴⁶ E. Rogers,²⁵ S. Rolli,⁵⁷ R. Roser,¹⁸ M. Rossi,^{55a} R. Rossin,¹¹ P. Roy,³⁴ A. Ruiz,¹² J. Russ,¹³ V. Rusu,¹⁸ B. Rutherford,¹⁸ H. Saarikko,²⁴ A. Safonov,⁵⁴ W. K. Sakumoto,⁵⁰ L. Santi,^{55b,55a} L. Sartori,^{47a} K. Sato,⁵⁶ A. Savoy-Navarro,⁴⁵ P. Schlabach,¹⁸ A. Schmidt,²⁷ E. E. Schmidt,¹⁸ M. A. Schmidt,¹⁴ M. P. Schmidt,^{61,a} M. Schmitt,³⁹ T. Schwarz,⁸ L. Scodellaro,¹² A. Scribano,^{47c,47a} F. Scuri,^{47a} A. Sedov,⁴⁹ S. Seidel,³⁸ Y. Seiya,⁴² A. Semenov,¹⁶ L. Sexton-Kennedy,¹⁸ F. Sforza,^{47b,47a} A. Sfyrla,²⁵ S. Z. Shalhout,⁵⁹ T. Shears,³⁰ P. F. Shepard,⁴⁸ M. Shimojima,^{56,u} S. Shiraishi,¹⁴ M. Shochet,¹⁴ Y. Shon,⁶⁰ I. Shreyber,³⁷ A. Simonenko,¹⁶ P. Sinervo,³⁴ A. Sisakyan,¹⁶ A. J. Slaughter,¹⁸ J. Slaunwhite,⁴⁰ K. Sliwa,⁵⁷ J. R. Smith,⁸ F. D. Snider,¹⁸ R. Snihur,³⁴ A. Soha,¹⁸ S. Somalwar,⁵³ V. Sorin,⁴ T. Spreitzer,³⁴ P. Squillacioti,^{47c,47a} M. Stanitzki,⁶¹ R. St. Denis,²² B. Stelzer,³⁴ O. Stelzer-Chilton,³⁴ D. Stentz,³⁹ J. Strogas,³⁸ G. L. Strycker,³⁵ J. S. Suh,²⁸ A. Sukhanov,¹⁹ I. Suslov,¹⁶ A. Taffard,^{25,g} R. Takashima,⁴¹ Y. Takeuchi,⁵⁶ R. Tanaka,⁴¹ J. Tang,¹⁴ M. Tecchio,³⁵ P. K. Teng,¹ J. Thom,^{18,i} J. Thome,¹³ G. A. Thompson,²⁵ E. Thomson,⁴⁶ P. Tipton,⁶¹ P. Ttito-Guzmán,³² S. Tkaczyk,¹⁸ D. Toback,⁵⁴ S. Tokar,¹⁵ K. Tollefson,³⁶ T. Tomura,⁵⁶ D. Tonelli,¹⁸ S. Torre,²⁰ D. Torretta,¹⁸ P. Totaro,^{55b,55a} S. Tournear,⁴⁵ M. Trovato,^{47d,47a} S.-Y. Tsai,¹ Y. Tu,⁴⁶ N. Turini,^{47c,47a} F. Ukegawa,⁵⁶ S. Uozumi,²⁸ N. van Remortel,^{24,c} A. Varganov,³⁵ E. Vataga,^{47d,47a} F. Vázquez,^{19,o} G. Velev,¹⁸ C. Vellidis,³ M. Vidal,³² I. Vila,¹² R. Vilar,¹² M. Vogel,³⁸ I. Volobouev,^{29,x} G. Volpi,^{47b,47a} P. Wagner,⁴⁶ R. G. Wagner,² R. L. Wagner,¹⁸ W. Wagner,^{27,bb} J. Wagner-Kuhr,²⁷ T. Wakisaka,⁴² R. Wallny,⁹ S. M. Wang,¹ A. Warburton,³⁴ D. Waters,³¹ M. Weinberger,⁵⁴ J. Weinelt,²⁷ W. C. Wester III,¹⁸ B. Whitehouse,⁵⁷ D. Whiteson,^{46,g} A. B. Wicklund,² E. Wicklund,¹⁸ S. Wilbur,¹⁴ G. Williams,³⁴ H. H. Williams,⁴⁶ P. Wilson,¹⁸ B. L. Winer,⁴⁰ P. Wittich,^{18,i} S. Wolbers,¹⁸ C. Wolfe,¹⁴ H. Wolfe,⁴⁰ T. Wright,³⁵ X. Wu,²¹ F. Würthwein,¹⁰ S. Xie,³³ A. Yagil,¹⁰ K. Yamamoto,⁴² J. Yamaoka,¹⁷ U. K. Yang,^{14,s} Y. C. Yang,²⁸ W. M. Yao,²⁹ G. P. Yeh,¹⁸ K. Yi,^{18,p} J. Yoh,¹⁸ K. Yorita,⁵⁸ T. Yoshida,^{42,m} G. B. Yu,¹⁷ I. Yu,²⁸ S. S. Yu,¹⁸ J. C. Yun,¹⁸ A. Zanetti,^{55a} Y. Zeng,¹⁷ X. Zhang,²⁵ Y. Zheng,^{9,e} and S. Zucchelli^{6b,6a}

(CDF Collaboration)

¹*Institute of Physics, Academia Sinica, Taipei, Taiwan 11529, Republic of China*²*Argonne National Laboratory, Argonne, Illinois 60439*³*University of Athens, 157 71 Athens, Greece*⁴*Institut de Física d'Altes Energies, Universitat Autònoma de Barcelona, E-08193, Bellaterra (Barcelona), Spain*⁵*Baylor University, Waco, Texas 76798*^{6a}*Istituto Nazionale di Fisica Nucleare Bologna, I-40127 Bologna, Italy*^{6b}*University of Bologna, I-40127 Bologna, Italy*⁷*Brandeis University, Waltham, Massachusetts 02254*⁸*University of California, Davis, Davis, California 95616*⁹*University of California, Los Angeles, Los Angeles, California 90024*¹⁰*University of California, San Diego, La Jolla, California 92093*¹¹*University of California, Santa Barbara, Santa Barbara, California 93106*¹²*Instituto de Física de Cantabria, CSIC-University of Cantabria, 39005 Santander, Spain*¹³*Carnegie Mellon University, Pittsburgh, Pennsylvania 15213*¹⁴*Enrico Fermi Institute, University of Chicago, Chicago, Illinois 60637*¹⁵*Comenius University, 842 48 Bratislava, Slovakia; Institute of Experimental Physics, 040 01 Kosice, Slovakia*¹⁶*Joint Institute for Nuclear Research, RU-141980 Dubna, Russia*¹⁷*Duke University, Durham, North Carolina 27708*¹⁸*Fermi National Accelerator Laboratory, Batavia, Illinois 60510*¹⁹*University of Florida, Gainesville, Florida 32611*²⁰*Laboratori Nazionali di Frascati, Istituto Nazionale di Fisica Nucleare, I-00044 Frascati, Italy*²¹*University of Geneva, CH-1211 Geneva 4, Switzerland*²²*Glasgow University, Glasgow G12 8QQ, United Kingdom*²³*Harvard University, Cambridge, Massachusetts 02138*²⁴*Division of High Energy Physics, Department of Physics, University of Helsinki and Helsinki Institute of Physics, FIN-00014, Helsinki, Finland*²⁵*University of Illinois, Urbana, Illinois 61801*²⁶*The Johns Hopkins University, Baltimore, Maryland 21218*

²⁷*Institut für Experimentelle Kernphysik, Karlsruhe Institute of Technology, D-76131 Karlsruhe, Germany*

²⁸*Center for High Energy Physics: Kyungpook National University, Daegu 702-701, Korea; Seoul National University, Seoul 151-742, Korea; Sungkyunkwan University, Suwon 440-746, Korea; Korea Institute of Science and Technology Information, Daejeon 305-806, Korea; Chonnam National University, Gwangju 500-757, Korea; Chonbuk National University, Jeonju 561-756, Korea*

²⁹*Ernest Orlando Lawrence Berkeley National Laboratory, Berkeley, California 94720*

³⁰*University of Liverpool, Liverpool L69 7ZE, United Kingdom*

³¹*University College London, London WC1E 6BT, United Kingdom*

³²*Centro de Investigaciones Energeticas, Medioambientales y Tecnológicas, E-28040 Madrid, Spain*

³³*Massachusetts Institute of Technology, Cambridge, Massachusetts 02139*

³⁴*Institute of Particle Physics: McGill University, Montréal, Québec, Canada H3A 2T8; Simon Fraser University, Burnaby, British Columbia, Canada V5A 1S6;*

University of Toronto, Toronto, Ontario, Canada M5S 1A7; and TRIUMF, Vancouver, British Columbia, Canada V6T 2A3

³⁵*University of Michigan, Ann Arbor, Michigan 48109*

³⁶*Michigan State University, East Lansing, Michigan 48824*

³⁷*Institution for Theoretical and Experimental Physics, ITEP, Moscow 117259, Russia*

³⁸*University of New Mexico, Albuquerque, New Mexico 87131*

³⁹*Northwestern University, Evanston, Illinois 60208*

⁴⁰*The Ohio State University, Columbus, Ohio 43210*

⁴¹*Okayama University, Okayama 700-8530, Japan*

⁴²*Osaka City University, Osaka 588, Japan*

⁴³*University of Oxford, Oxford OX1 3RH, United Kingdom*

^{44a}*Istituto Nazionale di Fisica Nucleare, Sezione di Padova-Trento, I-35131 Padova, Italy*

^{44b}*University of Padova, I-35131 Padova, Italy*

⁴⁵*LPNHE, Universite Pierre et Marie Curie/IN2P3-CNRS, UMR7585, Paris, F-75252 France*

⁴⁶*University of Pennsylvania, Philadelphia, Pennsylvania 19104*

^{47a}*Istituto Nazionale di Fisica Nucleare Pisa, I-56127 Pisa, Italy*

^{47b}*University of Pisa, I-56127 Pisa, Italy*

^{47c}*University of Siena, I-56127 Pisa, Italy*

^{47d}*Scuola Normale Superiore, I-56127 Pisa, Italy*

⁴⁸*University of Pittsburgh, Pittsburgh, Pennsylvania 15260*

⁴⁹*Purdue University, West Lafayette, Indiana 47907*

⁵⁰*University of Rochester, Rochester, New York 14627*

⁵¹*The Rockefeller University, New York, New York 10021*

^aDeceased

^bWith visitors from University of Massachusetts Amherst, Amherst, Massachusetts 01003

^cWith visitors from Universiteit Antwerpen, B-2610 Antwerp, Belgium

^dWith visitors from University of Bristol, Bristol BS8 1TL, United Kingdom

^eWith visitors from Chinese Academy of Sciences, Beijing 100864, China

^fWith visitors from Istituto Nazionale di Fisica Nucleare, Sezione di Cagliari, 09042 Monserrato (Cagliari), Italy

^gWith visitors from University of California Irvine, Irvine, California 92697

^hWith visitors from University of California Santa Cruz, Santa Cruz, California 95064

ⁱWith visitors from Cornell University, Ithaca, New York 14853

^jWith visitors from University of Cyprus, Nicosia CY-1678, Cyprus

^kWith visitors from University College Dublin, Dublin 4, Ireland

^lWith visitors from University of Edinburgh, Edinburgh EH9 3JZ, United Kingdom

^mWith visitors from University of Fukui, Fukui City, Fukui Prefecture, Japan 910-0017

ⁿWith visitors from Kinki University, Higashi-Osaka City, Japan 577-8502

^pWith visitors from University of Iowa, Iowa City, Iowa 52242

^qWith visitors from Kansas State University, Manhattan, Kansas 66506

^rWith visitors from Queen Mary, University of London, London, E1 4NS, United Kingdom

^sWith visitors from University of Manchester, Manchester M13 9PL, United Kingdom

^tWith visitors from Muons, Inc., Batavia, Illinois 60510

^uWith visitors from Nagasaki Institute of Applied Science, Nagasaki, Japan

^vWith visitors from University of Notre Dame, Notre Dame, Indiana 46556

^wWith visitors from University de Oviedo, E-33007 Oviedo, Spain

^xWith visitors from Texas Tech University, Lubbock, Texas 79609

^yWith visitors from IFIC(CSIC-Universitat de Valencia), 56071 Valencia, Spain

^zWith visitors from Universidad Tecnica Federico Santa Maria, 110v Valparaiso, Chile

^{aa}With visitors from University of Virginia, Charlottesville, Virginia 22906

^{bb}With visitors from Bergische Universität Wuppertal, 42097 Wuppertal, Germany

^{cc}With visitors from Yarmouk University, Irbid 211-63, Jordan

^{dd}With visitors from, on leave from J. Stefan Institute, Ljubljana, Slovenia

^{52a}*Istituto Nazionale di Fisica Nucleare, Sezione di Roma 1, I-00185 Roma, Italy*^{52b}*Sapienza Università di Roma, I-00185 Roma, Italy*⁵³*Rutgers University, Piscataway, New Jersey 08855*⁵⁴*Texas A&M University, College Station, Texas 77843*^{55a}*Istituto Nazionale di Fisica Nucleare Trieste/Udine, I-34100 Trieste, I-33100 Udine, Italy*^{55b}*University of Trieste/Udine, I-33100 Udine, Italy*⁵⁶*University of Tsukuba, Tsukuba, Ibaraki 305, Japan*⁵⁷*Tufts University, Medford, Massachusetts 02155*⁵⁸*Waseda University, Tokyo 169, Japan*⁵⁹*Wayne State University, Detroit, Michigan 48201*⁶⁰*University of Wisconsin, Madison, Wisconsin 53706*⁶¹*Yale University, New Haven, Connecticut 06520*

(Received 20 October 2009; published 21 December 2009)

A measurement of the cross section for the inclusive production of isolated photons by the CDF experiment at the Fermilab Tevatron collider is presented. The measurement covers the pseudorapidity region $|\eta^\gamma| < 1.0$ and the transverse energy range $E_T^\gamma > 30$ GeV and is based on 2.5 fb^{-1} of integrated luminosity. The sample is almost a factor of 7 larger than those used for recent published results and extends the E_T^γ coverage by 100 GeV. The result agrees with next-to-leading order perturbative QCD calculations within uncertainties over the range $50 < E_T^\gamma < 400$ GeV, though the energy spectrum in the data shows a steeper slope at lower E_T^γ .

DOI: 10.1103/PhysRevD.80.111106

PACS numbers: 13.85.Qk, 12.38.Qk

The measurement of inclusive prompt-photon production constitutes a test of perturbative QCD (pQCD) with the potential to constrain parton distribution functions (PDF), while avoiding the complications of jet identification and energy measurements. The photon cross section is also sensitive to the presence of new physics at large photon transverse energy. In high-energy $p\bar{p}$ collisions, photons are mostly produced via quark-gluon Compton scattering or quark-antiquark annihilation. In addition to these processes, photons can also be produced through the fragmentation of outgoing partons, though this contribution is reduced when the photon is required to be isolated from other particles in the final state. An isolation requirement is necessary to suppress the background from energetic π^0 and η mesons.

Previous experiments have presented results on inclusive prompt photon production compared to next-to-leading-order (NLO) pQCD predictions [1–4]. In this paper, we present a new measurement of the inclusive cross section based on 2.5 fb^{-1} of integrated luminosity collected by the CDF II detector at the Tevatron. Photons are required to be isolated, have a pseudorapidity $|\eta^\gamma| < 1.0$, and a transverse energy $E_T^\gamma > 30$ GeV [5]. This measurement extends the E_T^γ coverage by 100 GeV compared to previous measurements [4], and presents reduced systematic uncertainties as a result of using an improved background subtraction method based on the shape of the isolation distribution.

The CDF II detector [6] is a general-purpose particle detector located at the Tevatron collider. The charged-particle tracking system is immersed in a 1.4 T magnetic field aligned coaxially with the beam line, and provides tracking coverage in the pseudorapidity range $|\eta| \leq 2.0$. A

central preradiator detector surrounds the tracking system and samples the electromagnetic showers that begin in the material in front of it. This detector consisted of multiwire proportional chambers at the beginning of Run II, and was upgraded to scintillation tiles in 2004. Scintillator-based electromagnetic (EM) and hadronic (HAD) calorimeters arranged in projective towers of size $\Delta\eta \times \Delta\phi = 0.1 \times 0.26$ provide a coverage of $|\eta| < 3.6$. The energy resolution of the CEM calorimeters for photons and electrons is $\sigma/E_T = 13.5\%/\sqrt{E_T} \oplus 2\%$, where \oplus represents sum in quadrature. The central ($|\eta| < 1.1$) electromagnetic strip chambers (CES) are multiwire proportional chambers embedded inside the EM calorimeter and positioned at a depth corresponding to the expected maximum of the longitudinal shower profile (6 radiation lengths). Anode wires and cathode strips measure ϕ and z respectively, providing a 2 mm position resolution in each direction for 50 GeV electrons.

The data are collected using a three-level online event selection system (trigger) that selects events with at least one energy cluster consistent with a photon in the final state. A photon cluster consists of one to three consecutive calorimeter towers in the η direction. Photons are collected with two trigger thresholds in E_T^γ , 25 GeV and 70 GeV. In order to reduce contamination from neutral meson decays, the low E_T^γ trigger requires photon clusters to be isolated. The isolation requirement at the second level uses a simple box patterns of towers, while at the third level the extra energy inside a cone of radius $R = \sqrt{(\Delta\phi)^2 + (\Delta\eta)^2} = 0.4$ around the cluster is required to be less than 10% of the energy of the cluster (E^{clu}). The low E_T^γ trigger also requires the lateral shower profile of the CES cluster to be

consistent with that of electrons, as measured in test beam data.

The event selection requires the primary vertex z position to be within 60 cm of the center of the detector to maintain the projective nature of the calorimeter towers. In order to suppress beam-related backgrounds, cosmic rays, and calorimeter noise, as well as leptonic W decays [7], the missing transverse energy of the event has to be less than 80% of the transverse energy of the leading photon candidate. This requirement reduces these backgrounds to less than 1% each, while preserving almost 99% of the photon signal. Photon candidates are required to be matched to a photon cluster and to be fiducial to the CES detector. Photons with additional CES clusters are rejected, since contributions from neutral mesons occasionally produce multiple clusters. At most, one low transverse momentum track ($p_T^{\text{trk}} < 1 \text{ GeV}/c + 0.5\%E_T^\gamma/c$) is allowed to point to the photon candidate. The fraction of the energy of the photon in the hadronic calorimeter has to be small ($E^{\text{HAD}}/E^{\text{EM}} < 0.055 + 0.00045E^{\text{clu}}/\text{GeV}$), and, for events collected using the low E_T trigger, the CES shower associated with the photon candidate has to have a profile consistent with test beam electrons [8].

The transverse energy of the photon is corrected to account for nonuniformities in the calorimeter response, and calibrated using electrons from reconstructed Z bosons. Photon candidates are required to have $E_T^\gamma > 30 \text{ GeV}$ and to be isolated in the calorimeter, $E_T^{R=0.4} - E_T^\gamma = E_T^{\text{iso}} < 2 \text{ GeV}$, where $E_T^{R=0.4}$ is the transverse energy in a cone of $R = 0.4$ around the photon. The isolation requirement reduces the background from neutral mesons, but also suppresses the photon signal coming from parton fragmentation processes.

While the selection criteria remove the bulk of the neutral meson background, substantial contamination remains, mainly corresponding to fluctuations in the fragmentation of jets, leading to neutral mesons that carry most of the parton energy. To subtract these isolated π^0 and η mesons, the isolation distribution from the data (without the $E_T^{\text{iso}} < 2 \text{ GeV}$ requirement) is fitted with signal and background templates formed using Monte Carlo simulation. The isolation distribution is sensitive to the differences between prompt photons and background: photons produce a well-defined peak at low isolation while neutral mesons present a flatter shape. The signal template is obtained from a PYTHIA 6.216 [9] photon Monte Carlo sample and the background template is constructed by selecting photons from meson decays in a QCD PYTHIA sample. In both cases the underlying event model of PYTHIA is tuned to CDF jet data (TUNE A [10]). These events are passed through a GEANT [11] simulation of the detector and subjected to the same selection requirements as the data. As an example, Fig. 1 shows the isolation distribution in data compared to signal and background templates for photons in the region $70 < E_T^\gamma < 80 \text{ GeV}$.

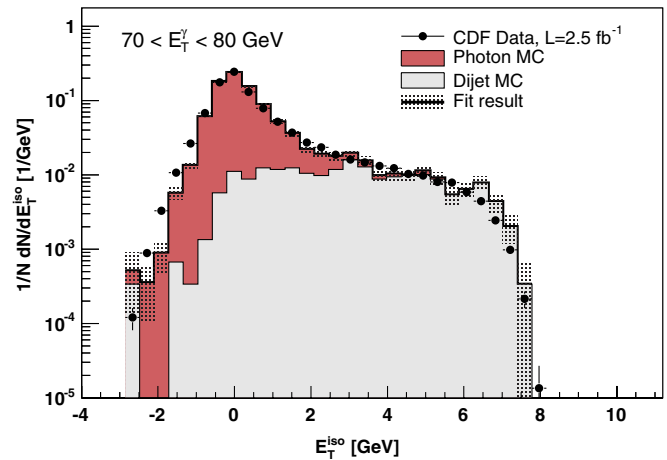


FIG. 1 (color online). Measured isolation distribution for photons with $70 < E_T^\gamma < 80 \text{ GeV}$. A χ^2 fit to the data (full points) with photon (dark histogram) and neutral mesons (light histogram) templates is used to extract the photon fraction. The result of the fit is shown as a full line with the associated uncertainty from the fitting procedure.

The raw E_T^{iso} is corrected for leakage effects and pile-up contributions which occasionally yield a negative E_T^{iso} , but if the negative E_T^{iso} bins are not included in the fit, the photon fraction changes by less than 2%. At high E_T^γ ($> 200 \text{ GeV}$) the signal template, as extracted from the Monte Carlo simulation, does not describe accurately the signal peak. This is attributed to deficiencies in the details of the shower simulation in the calorimeter and, to a lesser extent, to the model of the underlying event [12]. An E_T^γ -dependent correction is applied to modify the signal templates and improve the fitting process. At low E_T^γ no correction is necessary while at very high E_T^γ the template is shifted by -0.5 GeV and its width reduced by 50%. The correction, which is not applied to the background templates, only changes the final results by few percent, and is accounted for in the study of systematic uncertainties (see below). As a result of the fitting procedure, the photon fraction (\mathcal{F}) is extracted from the measured isolation distributions. Figure 2 shows the values for \mathcal{F} as a function of E_T^γ , including the systematic uncertainties discussed below.

The raw inclusive differential cross section as a function of E_T^γ is defined as $d\sigma/(dE_T^\gamma d\eta^\gamma) = (N^\gamma \mathcal{F})/(\Delta E_T^\gamma \Delta \eta^\gamma \epsilon_{\text{trig}} \mathcal{L})$, where N^γ is the number of photon candidates in a given E_T^γ bin, ΔE_T^γ ($\Delta \eta^\gamma$) is the size of the E_T^γ (η^γ) bin, ϵ_{trig} the trigger efficiency, and \mathcal{L} is the integrated luminosity. The trigger efficiency is approximately 100% in the kinematic region of the measurement. The measured cross section is corrected for acceptance, efficiency of the photon selection, and resolution effects back to the hadron level [13] using a bin-by-bin unfolding procedure and a sample of prompt-photon events simulated with PYTHIA. To avoid any bias on the unfolding factors due to assumptions about the true E_T^γ spectrum, the photon Monte Carlo sample is

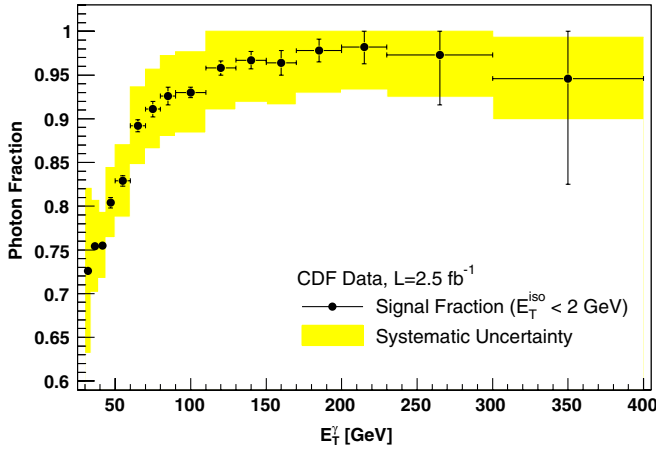


FIG. 2 (color online). Fraction of isolated prompt photons as a function of E_T^γ . The systematic uncertainty band is discussed in the text.

reweighted to match the measured spectrum. The resulting unfolding factors vary between 0.638 ± 0.003 and 0.69 ± 0.01 with little E_T^γ dependence.

A detailed study of systematic uncertainties is carried out [12]. The largest contribution to the total uncertainty at high E_T^γ is caused by the 1.5% uncertainty on the photon absolute energy scale, due to a small energy dependence in the energy ratio of simulated and data electrons from the Z mass peak. This introduces an uncertainty on the measured cross section that varies between 6% and 13% as E_T^γ increases. At low E_T^γ the dominant uncertainty source is the photon fraction. Different methods are considered to construct signal and background templates and extract \mathcal{F} : signal templates are defined using electrons from Z decays in data instead of using Monte Carlo simulated events; very simple templates (two bins in isolation) are considered, to remove the details of the isolation distribution in the fitting procedure; the photon signal is then extracted using background templates with and without the E_T^γ -dependent correction that is applied to the signal templates. In addition, a completely different method [8] based on the shower profile of the photon candidate in the CES detector and the number of conversions in the material in front of the preradiator detector is used to determine the neutral meson background. As a result, a conservative systematic uncertainty that varies between 13% at low E_T^γ and 5% at high E_T^γ (see Fig. 2) is assigned to the measured photon signal, covering the results from all the alternative methods. A 3% uncertainty on the measured cross section, approximately independent of E_T^γ , reflects uncertainties on the determination of the photon acceptance, and a 5% uncertainty on the measured cross section at low E_T^γ accounts for the uncertainty on the CES cut efficiency. An additional 10% uncertainty in the photon isolation energy introduces a 1% uncertainty on the measurement. Performing the unfolding procedure using unweighted Monte Carlo samples resulted in a less than 1% effect on the measured cross section. The

different sources of systematic uncertainty are added in quadrature. The total systematic uncertainty varies between 15% at low and very high E_T^γ , and 8% at intermediate E_T^γ . Finally, an additional 6% uncertainty due to the measurement of the integrated luminosity is considered [14].

The measured inclusive isolated prompt photon cross section as a function of E_T^γ is presented in Fig. 3 and Table I. The data are compared to NLO pQCD predictions as determined by the JETPHOX [15] program with CTEQ6.1M PDF [16], normalization, factorization and fragmentation scales set to E_T^γ , and photon isolation requirement as for the data. Variations of the scales by a factor of 2 change the prediction by 15% at low E_T^γ and 8% at high E_T^γ . The uncertainty on the predictions due to PDF varies between 4% at low E_T^γ and 13% at high E_T^γ , as determined using the Hessian method [17]. In addition, we have evaluated the theoretical prediction using the MRST04 [18] PDF, and find it well inside the experimental and other theoretical uncertainties.

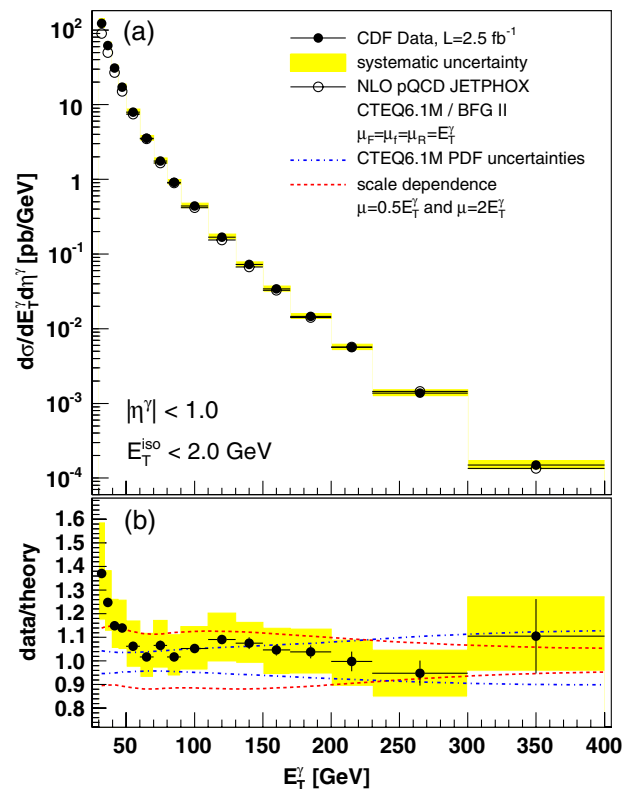


FIG. 3 (color online). (a) Measured inclusive isolated prompt-photon cross section as a function of E_T^γ compared to NLO pQCD predictions. (b) Ratio data/theory as a function of E_T^γ . The shaded band includes the total systematic uncertainty on the measurement except for the 6% luminosity uncertainty. The dashed and dotted lines indicate the PDF uncertainty and the variation with NLO pQCD predictions, respectively. A parton-to-hadron correction, $C_{\text{had}} = 0.91 \pm 0.03$, is applied to the theoretical predictions.

TABLE I. Measured inclusive isolated prompt photon cross section for photons in the pseudorapidity region $|\eta^\gamma| < 1.0$ and $30 < E_T^\gamma < 400$ GeV. The uncertainties in the central column are statistical. The additional 6% luminosity uncertainty is not included in the table. A parton-to-hadron correction ($C_{\text{had}} = 0.91 \pm 0.03$) is applied to the pQCD predictions.

E_T^γ (GeV)	$d\sigma/dE_T^\gamma d\eta^\gamma$ (pb/GeV)	Syst. Unc. (%)
30–34	$(1.23 \pm 0.01) \times 10^2$	+15.5, –14.5
34–39	$(6.21 \pm 0.03) \times 10^1$	+10.8, –9.8
39–44	$(3.10 \pm 0.02) \times 10^1$	+9.8, –8.4
44–50	$(1.72 \pm 0.02) \times 10^1$	+10.2, –8.1
50–60	$(7.93 \pm 0.08) \times 10^0$	+10.1, –8.4
60–70	$(3.54 \pm 0.05) \times 10^0$	+9.8, –8.5
70–80	$(1.76 \pm 0.03) \times 10^0$	+10.0, –9.1
80–90	$(9.08 \pm 0.14) \times 10^{-1}$	+9.3, –7.9
90–110	$(4.41 \pm 0.05) \times 10^{-1}$	+8.8, –8.7
110–130	$(1.68 \pm 0.03) \times 10^{-1}$	+8.6, –8.7
130–150	$(7.25 \pm 0.16) \times 10^{-2}$	+7.8, –8.0
150–170	$(3.41 \pm 0.08) \times 10^{-2}$	+8.8, –10.0
170–200	$(1.46 \pm 0.04) \times 10^{-2}$	+8.8, –9.1
200–230	$(5.66 \pm 0.24) \times 10^{-3}$	+9.0, –10.6
230–300	$(1.38 \pm 0.08) \times 10^{-3}$	+10.0, –10.7
300–400	$(1.49 \pm 0.21) \times 10^{-4}$	+15.2, –13.4

The theoretical prediction includes an additional correction factor, $C_{\text{had}}(E_T^\gamma)$, to account for the presence of non-pQCD contributions from the underlying event and fragmentation into hadrons, that tend to increase the energy in the isolation cone. C_{had} is estimated, using Monte Carlo generated events, as the ratio between the nominal E_T^γ distribution at the hadron level and the one obtained after turning off both the interactions between proton and anti-proton remnants and the string fragmentation in the Monte Carlo samples. Two different sets of tuned parameters in PYTHIA (TUNE A and DW [10]) are considered, and the mean effect $C_{\text{had}} = 0.91 \pm 0.03$, observed to have little E_T^γ dependence, is taken as the correction. The uncertainty on C_{had} covers the results obtained with the different PYTHIA tunes. As expected, the correction reduces the predicted cross section, since the presence of underlying event activity results in photons failing the isolation requirement.

A difference between data and the NLO pQCD predictions is observed for $E_T^\gamma < 50$ GeV. Discrepancies were also observed at low p_T in previous measurements at collider and fixed target experiments [1–3]. For $E_T^\gamma > 50$ GeV, good agreement is observed, and a global χ^2 test in this region, including correlations between systematic uncertainties across E_T^γ bins, finds a probability of 21%.

In conclusion, the measurement of the cross section for the inclusive production of isolated prompt photons with $30 < E_T^\gamma < 400$ GeV and $|\eta^\gamma| < 1.0$ in $p\bar{p}$ collisions at $\sqrt{s} = 1.96$ TeV, using data corresponding to an integrated luminosity of 2.5 fb^{-1} , has been presented. The sample is almost a factor of 7 larger than those used for recent published results [4] and extends the E_T^γ coverage by 100 GeV. A new method to determine the photon fraction based on the shape of the isolation distribution was implemented for the first time at CDF, which resulted in smaller uncertainties compared to previous results [1]. The measured cross section agrees with NLO pQCD predictions within uncertainties except at low E_T^γ where the data have a steeper slope.

We thank the Fermilab staff and the technical staffs of the participating institutions for their vital contributions. This work was supported by the U.S. Department of Energy and National Science Foundation; the Italian Istituto Nazionale di Fisica Nucleare; the Ministry of Education, Culture, Sports, Science and Technology of Japan; the Natural Sciences and Engineering Research Council of Canada; the National Science Council of the Republic of China; the Swiss National Science Foundation; the A.P. Sloan Foundation; the Bundesministerium für Bildung und Forschung, Germany; the World Class University Program, the National Research Foundation of Korea; the Science and Technology Facilities Council and the Royal Society, United Kingdom; the Institut National de Physique Nucleaire et Physique des Particules/CNRS; the Russian Foundation for Basic Research; the Ministerio de Ciencia e Innovación, and Programa Consolider-Ingenio 2010, Spain; the Slovak R&D Agency; and the Academy of Finland.

- [1] D. Acosta *et al.* (CDF Collaboration), Phys. Rev. D **65**, 112003 (2002).
 [2] V.M. Abazov *et al.* (DO Collaboration), Phys. Rev. Lett. **87**, 251805 (2001).
 [3] L. Apanasevich *et al.* (E706 Collaboration), Phys. Rev. Lett. **81**, 2642 (1998); G. Ballocci *et al.* (UA6 Collaboration), Phys. Lett. B **436**, 222 (1998); E. Annassontzis *et al.* (R806 Collaboration), Z. Phys. C **13**,

- 277 (1982); M Bonesini *et al.* (WA70 Collaboration), Z. Phys. C **38**, 371 (1988); C. Alba *et al.* (UA1 Collaboration), Phys. Lett. B **209**, 385 (1988); A.L.S. Angelis *et al.* (R110 Collaboration), Nucl. Phys. **B327**, 541 (1989); E. Anassontzis *et al.* (R807/AFS Collaboration), Sov. J. Nucl. Phys. **51**, 5 (1990); J. Alitti *et al.* (UA2 Collaboration), Phys. Lett. B **263**, 544 (1991); G. Ballocci *et al.* (UA6 Collaboration), Phys. Lett. B **436**,

T. AALTONEN *et al.*PHYSICAL REVIEW D **80**, 111106(R) (2009)

- 222 (1998).
- [4] V. M. Abazov *et al.* (DO Collaboration), Phys. Lett. B **639**, 151 (2006).
- [5] A cylindrical coordinate system with the z axis along the proton direction is used, in which θ is the polar angle. We define $E_T = E \sin\theta$, $p_T = p \sin\theta$, and pseudorapidity $\eta = -\ln(\tan(\theta/2))$. The missing transverse energy is defined by $\cancel{E}_T = -\sum_i E_T^i \hat{n}_i$, where i is the calorimeter tower number and \hat{n}_i is a unit vector perpendicular to the beam axis and pointing at the i th calorimeter tower. The missing transverse energy as measured by the calorimeters is corrected for jets and muons.
- [6] F. Abe *et al.*, Nucl. Instrum. Methods Phys. Res., Sect. A **271**, 387 (1988); D. Amidei *et al.*, Nucl. Instrum. Methods Phys. Res., Sect. A **350**, 73 (1994); F. Abe *et al.*, Phys. Rev. D **52**, 4784 (1995); P. Azzi *et al.*, Nucl. Instrum. Methods Phys. Res., Sect. A **360**, 137 (1995); The CDFII Detector Technical Design Report, Fermilab-Pub-96/390-E.
- [7] Cosmic rays may produce bremsstrahlung photons. Muons from beam-halo interactions with the beam pipe may in turn interact with the detector material producing photons. Electrons from W decays may fake photons if the associated track is not reconstructed. All these contributions lead to large missing transverse energy.
- [8] F. Abe *et al.* (CDF Collaboration), Phys. Rev. D **48**, 2998 (1993).
- [9] T. Sjöstrand *et al.*, Comput. Phys. Commun. **135**, 238 (2001).
- [10] R. Field, FERMILAB-CONF-06-408-E, FNAL, 2005.T. Affolder *et al.* (CDF Collaboration), Phys. Rev. D **65**, 092002 (2002).
- [11] R. Brun and F. Carminati, CERN, Programming Library Long Writeup W5013, 1993.
- [12] C. Deluca, Ph.D. thesis, U.A.B., Barcelona, 2009.
- [13] The hadron level in the Monte Carlo generators is defined using all final-state particles with lifetimes above 10^{-11} s.
- [14] D. Acosta *et al.*, Nucl. Instrum. Methods Phys. Res., Sect. A **494**, 57 (2002); S. Klimenko, J. Konigsberg, and T. M. Liss, FERMILAB-FN-0741, 2003.
- [15] S. Catani *et al.*, J. High Energy Phys. 05 (2002) 028.
- [16] J. Pumplin *et al.*, J. High Energy Phys. 07 (2002) 012.
- [17] J. Pumplin *et al.*, Phys. Rev. D **65**, 014013 (2001).
- [18] A.D. Martin, R.G. Roberts, W.J. Stirling, and R.S. Thorne, Phys. Lett. B **604**, 61 (2004).